

# Continuous-time subspace identification in closed-loop

Marco Bergamasco and Marco Lovera

**Abstract**—This paper deals with the problem of continuous-time model identification and presents a subspace-based algorithm capable of dealing with data generated by systems operating in closed-loop. The algorithm is developed by reformulating the identification problem from the continuous-time model to an equivalent one to which discrete-time subspace identification techniques can be applied. More precisely, the considered approach corresponds to the projection of the input-output data onto an orthonormal basis, defined in terms of Laguerre filters. In this framework, the PBSID subspace identification algorithm, originally developed in the case of discrete-time systems, can be reformulated for the continuous-time case. Simulation results are used to illustrate the achievable performance of the proposed approach with respect to existing methods available in the literature.

## I. INTRODUCTION

System identification is today a very mature research area, the results of which find application in a very diverse range of fields. While most of the literature on system identification focuses on discrete-time models, in many situations of practical interest (such, as, e.g., aircraft and rotorcraft identification, see for example [9], [16]) the direct estimation of the parameters of a continuous-time model from sampled input-output data is an important problem, for which dedicated methods and tools have to be developed. Moreover, the problem of identifying models under special circumstances which turn out to be critical in discrete-time, such as the identification of stiff systems, the use of non-equidistantly sampled data or special types of non-linear models make it necessary to develop special algorithms that can deal with these cases. The development of identification methods for continuous-time models is a challenge of its own, and has been studied extensively (see, e.g., the recent monograph [4] and the references therein).

In the last twenty years or so, Subspace Model Identification (SMI) algorithms have been developed, which have proven extremely successful in dealing with the estimation of discrete-time state space models for MIMO systems. Not surprisingly, the problem of extending SMI methods to the identification of continuous-time systems has been studied in a number of contributions. In [17] a frequency-domain approach to subspace identification of continuous-time models was proposed, while a time-domain SMI algorithm able to identify a continuous-time model from sampled input-output data was first proposed in [5], building on the framework introduced in [8]. More precisely, in the cited thesis the

MIMO Output-Error State sPace (MOESP, see [18]) class of SMI algorithms was extended to the identification of continuous-time models through the use of Laguerre filters: this allowed the development of a method that deals with noise in a similar way as its discrete-time counterparts. More recently, in [13] the version of the MOESP algorithm presented in [19], [20] is adopted and a discrete-time algebraic equation is derived starting from sampled input-output data by describing derivatives of stochastic processes in the distribution sense, while in [1], [11] the combination of the MOESP algorithm with filtering methods to avoid the need to compute numerical derivatives of input-output signals was proposed. In [15] a novel approach to the problem of continuous-time SMI has been presented, based on the adoption of orthonormal basis functions to arrive, again, at a PO-MOESP-like data equation for a continuous-time system.

All the above mentioned contributions, however, assume that the system under study is operating in open-loop. This assumption is frequently restrictive in practice and is typically violated, for example, in the above mentioned aerospace applications, in which partial loop closures must be retained during identification experiments, primarily for safety issues. The problem of closed-loop SMI has been studied extensively in recent years due to its high relevance for practical applications (see, e.g., [10], [3], [2], [7] and the references therein). The present state-of-the-art is represented by the so-called PBSID algorithm (see, again, [2]) which, under suitable assumptions, can provide consistent estimates of the state space matrices for a discrete-time, linear time-invariant system operating under feedback. To the best knowledge of the Authors, the problem of closed-loop subspace identification in continuous-time has been only considered in the literature in [12], where the application of the errors-in-variables approach of [3] is proposed to deal with correlation in a continuous-time setting.

In the light of the above discussion, the aim of this paper is to propose a novel continuous-time SMI scheme, based on the derivation of a PBSID-like algorithm within the all-pass domain proposed in [15] and relying on Laguerre projections of the sampled input-output data. The performance of the proposed approach with respect to existing algorithms will be demonstrated in a simulation study.

The paper is organised as follows: Section II provides a concise statement of the continuous-time SMI problem, while the proposed approach, together with the relevant background, is presented in detail in Sections III and IV. Simulation results are presented and discussed in Section V.

Paper supported by the Italian MIUR project Identification and Adaptive Control of Industrial Systems. The Authors are with the Dipartimento di Elettronica e Informazione, Politecnico di Milano, Milano, Italy. {bergamasco,lovera}@elet.polimi.it

## II. PROBLEM STATEMENT AND PRELIMINARIES

Consider the linear, time-invariant continuous-time system

$$\begin{aligned} dx(t) &= Ax(t)dt + Bu(t) + dw(t), \quad x(0) = x_0 \\ dz(t) &= Cx(t) + Du(t) + dv(t) \\ y(t)dt &= dz(t) \end{aligned} \quad (1)$$

where  $x \in \mathbb{R}^n$ ,  $u \in \mathbb{R}^m$  and  $y \in \mathbb{R}^p$  are, respectively, the state, input and output vectors and  $w \in \mathbb{R}^n$  and  $v \in \mathbb{R}^p$  are the process and the measurement noise, respectively, modelled as Wiener processes with incremental covariance given by

$$E \left\{ \begin{bmatrix} dw(t) \\ dv(t) \end{bmatrix} \begin{bmatrix} dw(t) \\ dv(t) \end{bmatrix}^T \right\} = \begin{bmatrix} Q & S \\ S^T & R \end{bmatrix} dt.$$

The system matrices  $A$ ,  $B$ ,  $C$  and  $D$ , of appropriate dimensions, are such that  $(A, C)$  is observable,  $(A, [B, Q^{1/2}])$  is controllable and  $A$ ,  $(A - KC)$  are asymptotically stable,  $K$  being the Kalman gain associated with the system. Assume that a dataset  $\{u(t_i), y(t_i)\}$ ,  $i \in [1, N]$  of sampled input/output data (possibly associated with a non equidistant sequence of sampling instants) obtained from system (1) is available. Then, the problem is to provide a consistent estimate of the state space matrices  $A$ ,  $B$ ,  $C$  and  $D$  (up to a similarity transformation) and of the Kalman gain  $K$ .

In the following Sections a number of definitions will be used, which are summarised hereafter for the sake of clarity. See, e.g., [23], [14] for further details.

Let  $\mathcal{L}_2(0, \infty)$  denote the space of square integrable and Lebesgue measurable functions of time  $0 < t < \infty$ , with the inner product defined as  $\langle f, g \rangle = \int_0^\infty f(t)g(t)dt$ , for  $f, g \in \mathcal{L}_2(0, \infty)$ ; the space  $\mathcal{H}_2$  is the closed subspace of  $\mathcal{L}_2(i\mathbb{R})$  with functions analytic in the open right half plane, with norm

$$\|U\|_2^2 = \sup_{\sigma > 0} \frac{1}{2\pi} \int_{-\infty}^{\infty} |U(\sigma + j\omega)|^2 d\omega = \frac{1}{2\pi} \int_{-\infty}^{\infty} |U(j\omega)|^2 d\omega. \quad (2)$$

In view of Parseval's relation, the spaces  $\mathcal{L}_2(0, \infty)$  and  $\mathcal{H}_2$  are related by the isometric isomorphism defined by the bilateral Fourier transform, so if  $U \in \mathcal{H}_2$ , the inverse Fourier transform  $u = \mathcal{F}^{-1}[U]$  is in  $\mathcal{L}_2(0, \infty)$  and  $\|U\|_2 = \|u\|_2$ .

A scalar transfer function  $w(s)$  is called inner if it is a bounded analytic function in the open right half plane (i.e.,  $w(j\omega) \in \mathcal{H}_\infty$ ), such that  $|w(j\omega)| = 1$  or  $w^\sim(j\omega)w(j\omega) = 1$  almost everywhere on the imaginary axis, where  $w^\sim(j\omega) = w^T(-j\omega)$  is the para-conjugate (i.e.,  $w$  is an all-pass transfer function). We further denote by  $\Lambda_w$  the multiplication operator  $L^2(0, \infty) \mapsto L^2(0, \infty)$  defined as

$$\Lambda_w u(t) = \mathcal{F}^{-1}[w\mathcal{F}[u(t)]]. \quad (3)$$

In the following the focus will be on the first order inner function

$$w(s) = \frac{s - a}{s + a}, \quad (4)$$

$a > 0$ , together with the associated realisation

$$w(s) = \frac{c_w b_w}{s - a_w} + d_w, \quad (5)$$

where  $a_w = -a$ ,  $b_w = -\sqrt{2a}$ ,  $c_w = \sqrt{2a}$ ,  $d_w = 1$ . Then, it can be shown that  $w(s)\mathcal{H}_2$  is a proper closed subspace of  $\mathcal{H}_2$ , the orthogonal complement of which is denoted as  $S = \mathcal{H}_2 \ominus w(s)\mathcal{H}_2$ , that

$$\mathcal{L}_0(s) = \frac{c_w}{s + a} = \frac{\sqrt{2a}}{s + a} \quad (6)$$

is a basis of the (one-dimensional) subspace  $S$  and that the set

$$\{\mathcal{L}_0, w\mathcal{L}_0, \dots, w^i\mathcal{L}_0, \dots\} \quad (7)$$

is an orthonormal basis of  $\mathcal{H}_2$ , i.e.,  $\mathcal{H}_2 = \bigoplus_{i=0}^{\infty} w^i S$ . Equivalently, letting  $l_0 = \mathcal{F}^{-1}[\mathcal{L}_0]$ , the set

$$\{l_0, \dots, \Lambda_w l_0, \Lambda_w^i l_0, \dots\} \quad (8)$$

is an orthonormal basis of  $\mathcal{L}_2(0, \infty)$ , i.e.,  $\mathcal{L}_2(0, \infty) = \bigoplus_{i=0}^{\infty} \Lambda_w^i S$ .

The Laguerre basis and its generalisations to wider classes of orthonormal basis functions (see, e.g., the classical references ([21], [22], [6]) have been used extensively in the system identification literature in order to formulate the system identification problem for continuous-time input-output models as a linear-in-the-parameters one. In this work, however, the properties of the Laguerre basis will be exploited in a different way, i.e., with the goal of converting continuous-time models into equivalent discrete-time ones, as discussed in the following Sections.

## III. FROM CONTINUOUS-TIME TO DISCRETE-TIME USING LAGUERRE FILTERS

The main issue in the application of SMI methods to continuous-time systems is the need of computing the high order derivatives of input-output measurements arising from the continuous-time data equation. This problem has been faced in the literature using a number of different approaches; in this paper we will rely on results first presented in [15], [14], which allow to obtain a discrete-time equivalent model starting from the continuous-time system (1), along the following lines. First note that under the assumptions stated in Section II, (1) can be written in innovation form as

$$\begin{aligned} dx(t) &= Ax(t)dt + Bu(t)dt + Kde(t) \\ dz(t) &= Cx(t)dt + Du(t)dt + de(t) \\ y(t)dt &= dz(t). \end{aligned} \quad (9)$$

Under the assumptions stated in Section II, the system (9) is asymptotically stable, so it is possible to apply the results of [15] to derive a discrete-time equivalent model, as follows. Consider the first order inner function  $w(s)$  defined in (4) and apply to the input  $u$ , the output  $y$  and the innovation  $e$  of (9) the transformations

$$\begin{aligned} \tilde{u}(k) &= \int_0^\infty \Lambda_w^k v(t)u(t)dt \\ \tilde{y}(k) &= \int_0^\infty \Lambda_w^k v(t)y(t)dt \\ \tilde{e}(k) &= \int_0^\infty \Lambda_w^k v(t)e(t)dt, \end{aligned} \quad (10)$$

where  $\tilde{u}(k) \in \mathbb{R}^m$ ,  $\tilde{e}(k) \in \mathbb{R}^p$  and  $\tilde{y}(k) \in \mathbb{R}^p$ . Then (see [15] for details) the transformed system has the state space representation

$$\begin{aligned}\xi(k+1) &= A_o \xi(k) + B_o \tilde{u}(k) + K_o \tilde{e}(k), \quad \xi(0) = 0 \\ \tilde{y}(k) &= C_o \xi(k) + D_o \tilde{u}(k) + \tilde{e}(k)\end{aligned}\quad (11)$$

where the state space matrices are given by

$$\begin{aligned}A_o &= (A - aI)^{-1}(A + aI) \\ B_o &= \sqrt{2a}(A - aI)^{-1}B \\ K_o &= \sqrt{2a}(A - aI)^{-1}K \\ C_o &= -\sqrt{2a}C(A - aI)^{-1} \\ D_o &= \bar{D} - C(A - aI)^{-1}B.\end{aligned}\quad (12)$$

#### IV. CONTINUOUS-TIME PREDICTOR-BASED SUBSPACE MODEL IDENTIFICATION

On the basis of the approach described in the previous Section to the derivation of a discrete-time equivalent model for the system (1), in this Section a continuous-time subspace model identification algorithm based on the predictor-based idea first proposed in [2] is presented and discussed.

Considering the sequence of sampling instants  $t_i$ ,  $i = 1, \dots, N$ , the input  $u$ , the output  $y$  and the innovation  $e$  of (9) are subjected to the transformations

$$\begin{aligned}\tilde{u}_i(k) &= \int_0^\infty (\Lambda_w^k v(\tau))u(t_i + \tau)d\tau \\ \tilde{e}_i(k) &= \int_0^\infty (\Lambda_w^k v(\tau))e(t_i + \tau)d\tau \\ \tilde{y}_i(k) &= \int_0^\infty (\Lambda_w^k v(\tau))y(t_i + \tau)d\tau\end{aligned}\quad (13)$$

where  $\tilde{u}_i(k) \in \mathbb{R}^m$ ,  $\tilde{e}_i(k) \in \mathbb{R}^p$  and  $\tilde{y}_i(k) \in \mathbb{R}^p$ . Then (see [15] for details) the transformed system has the state space representation

$$\begin{aligned}\xi_i(k+1) &= A_o \xi_i(k) + B_o \tilde{u}_i(k) + K_o \tilde{e}_i(k), \quad \xi_i(0) = x(t_i) \\ \tilde{y}_i(k) &= C_o \xi_i(k) + D_o \tilde{u}_i(k) + \tilde{e}_i(k)\end{aligned}\quad (14)$$

where the state space matrices are given by (12).

Letting now

$$\tilde{z}_i(k) = [\tilde{u}_i^T(k) \quad \tilde{y}_i^T(k)]^T$$

and

$$\tilde{B}_o = [\bar{B}_o \quad K_o],$$

system (14) can be written as

$$\begin{aligned}\xi_i(k+1) &= \bar{A}_o \xi_i(k) + \tilde{B}_o \tilde{z}_i(k), \quad \xi_i(0) = x(t_i) \\ \tilde{y}_i(k) &= C_o \xi_i(k) + D_o \tilde{u}_i(k) + \tilde{e}_i(k),\end{aligned}\quad (15)$$

where

$$\begin{aligned}\bar{A}_o &= A_o - K_o C_o \\ \tilde{B}_o &= B_o - K_o D_o,\end{aligned}$$

to which the  $\text{PBSID}_{opt}$  algorithm can be applied, along the lines of the previous subsection, to compute estimates of the state space matrices  $A_o$ ,  $B_o$ ,  $C_o$ ,  $D_o$ ,  $K_o$ .

More precisely, iterating  $p-1$  times the state equation in (15) one gets

$$\begin{aligned}\xi_i(k+2) &= \bar{A}_o^2 \xi_i(k) + [\bar{A}_o \tilde{B}_o \quad \tilde{B}_o] \begin{bmatrix} \tilde{z}_i(k) \\ \tilde{z}_i(k+1) \end{bmatrix} \\ &\vdots \\ \xi_i(k+p) &= \bar{A}_o^p \xi_i(k) + \mathcal{K}^p Z_i^{0,p-1}\end{aligned}\quad (16)$$

where

$$\mathcal{K}^p = [\bar{A}_o^{p-1} \tilde{B}_o \quad \dots \quad \tilde{B}_o] \quad (17)$$

is the extended controllability matrix of the system in the transformed domain and

$$Z_i^{0,p-1} = \begin{bmatrix} \tilde{z}_i(k) \\ \vdots \\ \tilde{z}_i(k+p-1) \end{bmatrix}.$$

Under the considered assumptions,  $A_o$  has all the eigenvalues inside the open unit circle, so the term  $\bar{A}_o^p \xi_i(k)$  is negligible for sufficiently large values of  $p$  and we have that

$$\xi_i(k+p) \simeq \mathcal{K}^p Z_i^{0,p-1}.$$

As a consequence, the input-output behaviour of the system is approximately given by

$$\begin{aligned}\tilde{y}_i(k+p) &\simeq C_o \mathcal{K}^p Z_i^{0,p-1} + D_o \tilde{u}_i(k+p) + \tilde{e}_i(k+p) \\ &\vdots \\ \tilde{y}_i(k+p+f) &\simeq C_o \mathcal{K}^p Z_i^{f,p+f-1} + D_o \tilde{u}_i(k+p+f) + \tilde{e}_i(k+p+f),\end{aligned}\quad (18)$$

so that introducing the vector notation

$$\begin{aligned}Y_i^{p,f} &= [\tilde{y}_i(k+p) \quad \tilde{y}_i(k+p+1) \quad \dots \quad \tilde{y}_i(k+p+f)] \\ U_i^{p,f} &= [\tilde{u}_i(k+p) \quad \tilde{u}_i(k+p+1) \quad \dots \quad \tilde{u}_i(k+p+f)] \\ E_i^{p,f} &= [\tilde{e}_i(k+p) \quad \tilde{e}_i(k+p+1) \quad \dots \quad \tilde{e}_i(k+p+f)] \\ \Xi_i^{p,f} &= [\xi_i(k+p) \quad \xi_i(k+p+1) \quad \dots \quad \xi_i(k+p+f)] \\ \bar{Z}_i^{p,f} &= [Z_i^{0,p-1} \quad Z_i^{1,p} \quad \dots \quad Z_i^{f,p+f-1}]\end{aligned}$$

equations (16) and (18) can be rewritten as

$$\begin{aligned}\Xi_i^{p,f} &\simeq \mathcal{K}^p \bar{Z}_i^{p,f} \\ Y_i^{p,f} &\simeq C_o \mathcal{K}^p \bar{Z}_i^{p,f} + D_o U_i^{p,f} + E_i^{p,f}.\end{aligned}\quad (19)$$

Considering now the entire dataset for  $i = 1, \dots, N$ , the data matrices become

$$Y^{p,f} = \begin{bmatrix} \tilde{y}_1^T(k+p) \\ \vdots \\ \tilde{y}_N^T(k+p) \\ \vdots \\ \tilde{y}_1^T(k+p+f) \\ \vdots \\ \tilde{y}_N^T(k+p+f) \end{bmatrix}^T, \quad (20)$$

and similarly for  $U_i^{p,f}$ ,  $E_i^{p,f}$ ,  $\Xi_i^{p,f}$  and  $\bar{Z}_i^{p,f}$ . The data equations (19), in turn, are given by

$$\begin{aligned} \Xi^{p,f} &\simeq \mathcal{K}^p \bar{Z}^{p,f} \\ Y^{p,f} &\simeq C_o \mathcal{K}^p \bar{Z}^{p,f} + D_o U^{p,f} + E^{p,f}. \end{aligned} \quad (21)$$

From this point on, the algorithm can be developed along the lines of the discrete-time PBSID<sub>opt</sub> method, i.e., by carrying out the following steps. Considering  $p = f$ , estimates for the matrices  $C_o \mathcal{K}^p$  and  $D_o$  are first computed by solving the least-squares problem

$$\min_{C_o \mathcal{K}^p, D_o} \|Y^{p,p} - C_o \mathcal{K}^p \bar{Z}^{p,p} - D_o U^{p,p}\|_F. \quad (22)$$

Defining now the extended observability matrix  $\Gamma^p$  as

$$\Gamma^p = \begin{bmatrix} C_o \\ C_o \bar{A}_o \\ \vdots \\ C_o \bar{A}_o^{p-1} \end{bmatrix} \quad (23)$$

and noting that the product of  $\Gamma^p$  and  $\mathcal{K}^p$  can be written as

$$\begin{aligned} \Gamma^p \mathcal{K}^p &= \begin{bmatrix} C_o \bar{A}_o^{p-1} \tilde{B}_o & \dots & C_o \tilde{B}_o \\ C_o \bar{A}_o^p \tilde{B}_o & \dots & C_o \bar{A}_o \tilde{B}_o \\ \vdots & & \\ C_o \bar{A}_o^{2p-2} \tilde{B}_o & \dots & C_o \bar{A}_o^{p-1} \tilde{B}_o \end{bmatrix} \\ &\simeq \begin{bmatrix} C_o \bar{A}_o^{p-1} \tilde{B}_o & \dots & C_o \tilde{B}_o \\ 0 & \dots & C_o \bar{A}_o \tilde{B}_o \\ \vdots & & \\ 0 & \dots & C_o \bar{A}_o^{p-1} \tilde{B}_o \end{bmatrix}, \end{aligned} \quad (24)$$

such product can be computed using the estimate  $\widehat{C_o \mathcal{K}^p}$  of  $C_o \mathcal{K}^p$  obtained by solving the least squares problem (22).

Recalling now that

$$\Xi^{p,p} \simeq \mathcal{K}^p \bar{Z}^{p,p} \quad (25)$$

it also holds that

$$\Gamma^p \Xi^{p,p} \simeq \Gamma^p \mathcal{K}^p \bar{Z}^{p,p}. \quad (26)$$

Therefore, computing the singular value decomposition

$$\Gamma^p \mathcal{K}^p \bar{Z}^{p,p} = U \Sigma V^T \quad (27)$$

an estimate of the state sequence can be obtained as

$$\widehat{\Xi}^{p,p} = \Sigma_n V_n^T, \quad (28)$$

from which, in turn, an estimate of  $C_o$  can be computed by solving the least squares problem

$$\min_{C_o} \|Y^{p,p} - \widehat{D}_o U^{p,p} - C_o \widehat{\Xi}^{p,p}\|_F. \quad (29)$$

The final steps consist of the estimation of the innovation data matrix  $E_N^{p,f}$

$$E_N^{p,f} = Y^{p,p} - \widehat{C}_o \widehat{\Xi}^{p,p} - \widehat{D}_o U^{p,p} \quad (30)$$

and of the entire set of the state space matrices for the system in the transformed domain, which can be obtained by solving the least squares problem

$$\min_{A_o, B_o, K_o} \|\widehat{\Xi}^{p+1,p} - A_o \widehat{\Xi}^{p,p-1} - B_o U^{p,p-1} - K_o E^{p,p-1}\|_F. \quad (31)$$

Finally, the state space form for the original continuous-time system can be recovered by means of equations (12).

*Remark 1:* The proposed identification algorithm assumes that continuous-time projections of the input-output data on the Laguerre basis can be computed exactly. This is obviously not the case, so suitable discretisation schemes for the considered Laguerre projection operations must be devised. In this work, the approximate implementation

$$\begin{aligned} \tilde{u}_i(k) &= \int_0^\infty \Lambda_w^k v(\tau) u(t_i + \tau) d\tau = \\ &= \int_{t_i}^\infty \Lambda_w^k v(\tau - t_i) u(\tau) d\tau = \\ &\simeq \int_{t_i}^{t_{N/2+t_i}} \Lambda_w^k v(\tau - t_i) u(\tau) d\tau, \quad i = 1, \dots, \frac{N}{2}, \end{aligned} \quad (32)$$

and similarly for  $\tilde{y}_i(k)$ , has been adopted, in which the indefinite integral has to be computed over a sliding window of length equal to half of the duration of the available dataset. For this reason, in comparing algorithms based on this projection with algorithms based on other continuous-time SMI schemes (see Section V) longer experiments have been considered.

## V. SIMULATION EXAMPLES

The performance of the continuous-time SMI algorithm outlined in Section IV has been evaluated and compared with the one achieved by the continuous-time PO-MOESP algorithms presented, respectively, in [5] (and denoted in the following as PO-MOESP<sub>w</sub> and [15] (denoted in the following as PO-MOESP<sub>o</sub>) in three simulation examples in which input-output data have been collected from, respectively, a stable system operating in open-loop, a stable system operating in closed-loop and an unstable system operating in closed-loop. In all cases, the simulated data has been collected by applying to the system a sequence of filtered white Gaussian noise as input. White Gaussian noise of increasing variance has been added to the output in order to assess the influence of decreasing signal-to-noise ratio on the quality of the computed estimates. For the input and output variables two values of the sampling interval, namely  $\Delta t = 0.005$  s and  $\Delta t = 0.01$  s have been considered. The  $p$  and  $f$  parameters have been chosen as  $p = f = 10$  for the PO-MOESP<sub>w</sub> and PO-MOESP<sub>o</sub> while for the PBSID<sub>w</sub>  $p = f = 20$  has been used.

### A. Open-loop system

The open-loop system considered in the first example is given by the transfer function

$$G(s) = \frac{32}{(s+8)(s+2)}. \quad (33)$$

The first issue to be investigated is the role of the choice of the parameter of the Laguerre filter bank  $a$ , which is known to be a critical issue for the continuous-time PO-MOESP<sub>w</sub> algorithm of [5]. The results obtained repeating the identification exercise for values of  $a$  ranging between 1 and 50 are depicted in Figure 1. As can be seen from the figure, the algorithms provide very different results as a function of  $a$ : the bias on the estimates of the eigenvalues increases faster for the PO-MOESP<sub>o</sub> algorithm than for the other algorithms. On the other hand, over the, more reasonable, range between 10 and 30, the PBSID<sub>o</sub> algorithm leads to a consistently lower bias and also to a more regular behaviour of the estimation error with respect to the tuning of the Laguerre filters.

Similar comments apply to the variance of the estimated eigenvalues. First of all, the results confirm findings already present in the literature about the somewhat erratic behaviour of the estimates of PO-MOESP<sub>w</sub> as functions of  $a$ . The PO-MOESP<sub>o</sub> leads to large values of variance for increasing  $a$ . As for the PBSID<sub>o</sub> algorithm, the variance is significantly smaller, over a wide range of values of  $a$ .

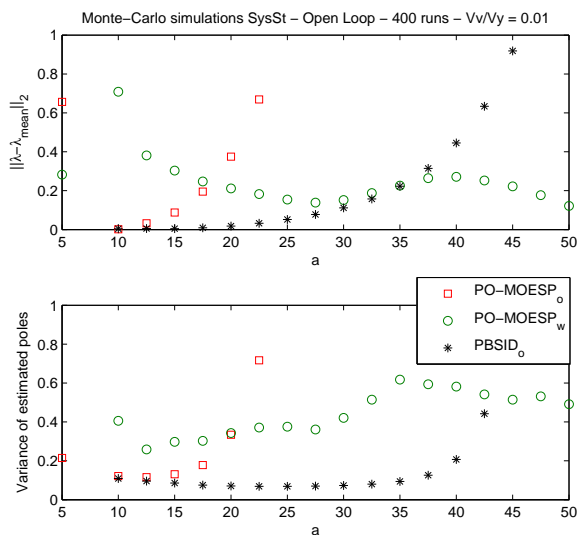


Fig. 1. Example 1: bias and variance of the estimated eigenvalues as functions of the Laguerre pole  $a$ .

A more detailed comparison between the performance of the algorithms can be carried out by looking at Tables I-II, where the results obtained in a Monte Carlo study (averaging over 400 runs, with  $a = 20$ ) are presented. More precisely, the estimation error for the eigenvalues of the system under study has been analysed for decreasing signal-to-noise ratio, as measured on the output. The Tables confirm in a more quantitative way the conclusions which were already drawn from the analysis of Figure 1. Note, in passing, that for low signal-to-noise ratio the continuous-time PO-MOESP<sub>w</sub> algorithm sometimes leads to complex estimates of the real eigenvalues, while the algorithms based on Laguerre projections always provide real estimates, even though the performance of PO-MOESP<sub>o</sub> is not satisfactory.

## B. Closed-loop system 1

The second considered example consists in the analysis of data generated by the system

$$G(s) = \frac{32}{(s+8)(s+2)}, \quad (34)$$

operating under feedback with the controller

$$R(s) = 2, \quad (35)$$

which in turn operates on the basis of noisy measurements of the output. The identification experiments have been carried out using, again, a sequence of filtered white Gaussian noise as input and adding white Gaussian noise of increasing variance to the output. The results obtained in this second example are summarised in Tables III-IV. As can be seen from the results, again algorithms based on Laguerre projections provide superior performance in terms of eigenvalue estimation accuracy, with PBSID<sub>o</sub> leading to smaller variance of the estimated eigenvalues with respect to POMOESP<sub>o</sub> and a reduced sensitivity of the performance to the choice of a larger sampling interval.

## C. Closed-loop system 2

The last example consists in the analysis of data generated by the (unstable) system

$$G(s) = \frac{8}{(s-2)(s+4)}, \quad (36)$$

operating under feedback with the controller

$$R(s) = 2, \quad (37)$$

which in turn operates on the basis of noisy measurements of the output. The obtained results are given in Tables V-VI. As can be seen from the Tables, conclusions similar to the ones drawn from the previous example can be obtained. This is somewhat surprising as, in principle, the operation of PBSID<sub>o</sub> requires the assumption that the open-loop system to be identified is asymptotically stable.

## VI. CONCLUDING REMARKS

In this paper, the problem of continuous-time model identification has been studied and a subspace-based algorithm has been proposed. The algorithm is based on the reformulation of the identification problem from continuous-time to discrete-time by using projections of the data onto the Laguerre basis for the appropriate signal space. In this framework, it has been shown that the PBSID<sub>opt</sub> subspace identification algorithm, originally developed in the case of discrete-time systems, can be reformulated for the continuous-time case. Future work will aim at a more detailed analysis of the effect of digital implementation of the algorithm on the accuracy of the estimates.

$\sigma_v^2/\sigma_y^2$	POMOESP <sub>w</sub>	POMOESP <sub>o</sub>	PBSID <sub>o</sub>
0.01	-0.1724 ± (0.5044)	0.3533 ± (0.4870)	0.0545 ± (0.2432)
	0.0164 ± (0.0550)	-0.0295 ± (0.0549)	-0.0037 ± (0.0295)
0.05	-0.9647 + 0.0279i ± (1.2864 + i0.2014)	0.3165 ± (0.7463)	0.0699 ± (0.5544)
	0.1262 - 0.0279i ± (0.2071 + i0.2014)	-0.0212 ± (0.0888)	-0.0010 ± (0.0688)
0.10	-1.9199 + 0.1507i ± (1.8298 + i0.4296)	0.1890 ± (0.9106)	-0.0055 ± (0.7789)
	0.2321 - 0.1507i ± (0.7014 + i0.4296)	-0.0038 ± (0.1156)	0.0115 ± (0.0962)

TABLE I

EXAMPLE 1: MEAN AND STANDARD DEVIATION OF THE EIGENVALUE ESTIMATION ERROR - OPEN-LOOP EXPERIMENTS WITH  $\Delta t = 0.005$  s.

$\sigma_v^2/\sigma_y^2$	POMOESP <sub>w</sub>	POMOESP <sub>o</sub>	PBSID <sub>o</sub>
0.01	-0.3483 ± (0.6854)	43.3117 ± (80.1747)	0.4807 ± (0.5340)
	0.0422 ± (0.0938)	-0.4774 ± (0.2729)	-0.0420 ± (0.0510)
0.05	-1.7846 + 0.1054i ± (1.6264 + i0.3573)	54.0676 ± (121.6504)	0.6155 ± (1.0860)
	0.2798 - 0.1054i ± (0.3466 + i0.3573)	-2.0905 ± (32.4239)	-0.0484 ± (0.0971)
0.10	-3.3825 + 0.5119i ± (2.0740 + i0.7093)	39.9113 ± (60.0398)	0.7604 ± (2.2822)
	0.3110 - 0.5119i ± (1.0086 + i0.7093)	-15.3255 ± (296.9840)	-0.0321 ± (0.1598)

TABLE II

EXAMPLE 1: MEAN AND STANDARD DEVIATION OF THE EIGENVALUE ESTIMATION ERROR - OPEN-LOOP EXPERIMENTS WITH  $\Delta t = 0.01$  s.

$\sigma_v^2/\sigma_y^2$	POMOESP <sub>w</sub>	POMOESP <sub>o</sub>	PBSID <sub>o</sub>
0.01	-0.0765 ± (0.3703)	0.0641 ± (0.2123)	0.0120 ± (0.1517)
	0.0134 ± (0.0733)	-0.0049 ± (0.0432)	-0.0023 ± (0.0354)
0.05	-0.3063 ± (0.7704)	0.0553 ± (0.3658)	0.0255 ± (0.3561)
	0.0628 ± (0.1675)	0.0005 ± (0.0809)	0.0019 ± (0.0774)
0.10	-0.7889 + 0.0224i ± (1.1853 + i0.1506)	0.0252 ± (0.5258)	-0.0108 ± (0.4980)
	0.1769 - 0.0224i ± (0.3273 + i0.1506)	0.0080 ± (0.1216)	0.0122 ± (0.1142)

TABLE III

EXAMPLE 2: MEAN AND STANDARD DEVIATION OF THE EIGENVALUE ESTIMATION ERROR - CLOSED-LOOP EXPERIMENTS WITH  $\Delta t = 0.005$  s.

$\sigma_v^2/\sigma_y^2$	POMOESP <sub>w</sub>	POMOESP <sub>o</sub>	PBSID <sub>o</sub>
0.01	-0.1211 ± (0.4337)	1.4571 ± (2.0238)	0.0532 ± (0.2193)
	0.0216 ± (0.0851)	-0.1122 ± (0.2022)	-0.0066 ± (0.0491)
0.05	-0.6860 + 0.0117i ± (1.1304 + i0.1004)	1.4221 ± (1.7205)	0.0461 ± (0.4784)
	0.1607 - 0.0117i ± (0.3226 + i0.1004)	-0.0960 ± (0.2153)	0.0039 ± (0.1171)
0.10	-1.3998 + 0.1097i ± (1.5445 + i0.3988)	1.3589 ± (1.9156)	0.0618 ± (0.6472)
	0.3230 - 0.1097i ± (0.4693 + i0.3988)	-0.0958 ± (0.2353)	-0.0031 ± (0.1508)

TABLE IV

EXAMPLE 2: MEAN AND STANDARD DEVIATION OF THE EIGENVALUE ESTIMATION ERROR - CLOSED-LOOP EXPERIMENTS WITH  $\Delta t = 0.01$  s.

$\sigma_v^2/\sigma_y^2$	POMOESP <sub>w</sub>	POMOESP <sub>o</sub>	PBSID <sub>o</sub>
0.01	-0.0190 ± (0.1276)	0.0588 ± (0.1008)	0.0315 ± (0.0688)
	0.0163 ± (0.0208)	0.0072 ± (0.0523)	0.0184 ± (0.0265)
0.05	-0.1002 ± (0.3100)	0.0558 ± (0.1823)	0.0446 ± (0.1606)
	0.0189 ± (0.0486)	0.0193 ± (0.0802)	0.0357 ± (0.0557)
0.10	-0.1636 ± (0.4567)	0.0380 ± (0.2497)	0.0561 ± (0.2337)
	0.0208 ± (0.0719)	0.0232 ± (0.1124)	0.0470 ± (0.0837)

TABLE V

EXAMPLE 3: MEAN AND STANDARD DEVIATION OF THE EIGENVALUE ESTIMATION ERROR - CLOSED-LOOP EXPERIMENTS WITH  $\Delta t = 0.005$  s.

$\sigma_v^2/\sigma_y^2$	POMOESP <sub>w</sub>	POMOESP <sub>o</sub>	PBSID <sub>o</sub>
0.01	0.0087 ± (0.1891)	0.7465 ± (1.0395)	0.0625 ± (0.1059)
	0.0291 ± (0.0311)	0.1304 ± (0.2394)	0.0591 ± (0.0394)
0.05	-0.1085 ± (0.4403)	0.6979 ± (1.0442)	0.0729 ± (0.2390)
	0.0288 ± (0.0740)	0.1709 ± (0.3444)	0.0895 ± (0.0874)
0.10	-0.2842 ± (0.6547)	0.8236 + 0.0016i ± (1.2856 + i0.0324)	0.0998 ± (0.3227)
	0.0433 ± (0.1179)	0.2679 - 0.0016i ± (0.5145 + i0.0324)	0.1174 ± (0.1287)

TABLE VI

EXAMPLE 3: MEAN AND STANDARD DEVIATION OF THE EIGENVALUE ESTIMATION ERROR - CLOSED-LOOP EXPERIMENTS WITH  $\Delta t = 0.01$  s.

## REFERENCES

- [1] T. Bastogne, H. Garnier, and P. Sibille. A PMF-based subspace method for continuous-time model identification. application to a multivariable winding process. *International Journal of Control*, 74(2):118–132, 2001.
- [2] A. Chiuso and G. Picci. Consistency analysis of certain closed-loop subspace identification methods. *Automatica*, 41(3):377–391, 2005.
- [3] C.T. Chou and M. Verhaegen. Subspace algorithms for the identification of multivariable dynamic error-in-variables state space models. *Automatica*, 33(10):1857–1869, 1997.
- [4] H. Garnier and L. Wang, editors. *Identification of continuous-time models from sampled data*. Springer, 2008.
- [5] B. R. J. Haverkamp. *State space identification: theory and practice*. PhD thesis, Delft University of Technology, 2001.
- [6] P. S. C. Heuberger, P. M. J. Van den Hof, and O. H. Bosgra. A generalized orthonormal basis for linear dynamical systems. *IEEE Transactions on Automatic Control*, 40(5):451–465, 2005.
- [7] B. Huang, S.X. Ding, and S.J. Qin. Closed-loop subspace identification: an orthogonal projection approach. *Journal of Process Control*, 15(1):53–66, 2005.
- [8] R. Johansson, M. Verhaegen, and C.T. Chou. Stochastic theory of continuous-time state-space identification. *IEEE Transactions on Signal Processing*, 47(1):41–51, 1999.
- [9] V. Klein and E.A. Morelli. *Aircraft System Identification: Theory And Practice*. AIAA, 2006.
- [10] L. Ljung and T. McKelvey. Subspace identification from closed loop data. *Signal Processing*, 52(2):209–215, 1996.
- [11] G. Mercère, R. Ouvrard, M. Gilson, and H. Garnier. Identification de systèmes multivariés à temps continu par approche des sous-espaces. *Journal Européen des Systèmes Automatisés*, 42(2-3):261–285, 2008.
- [12] R. Mohd-Moktar and L. Wang. Continuous time state space model identification using closed-loop data. In *Second Asia International Conference on Modelling & Simulation, Kuala Lumpur, Malaysia*, 2008.
- [13] A. Ohsumi, K. Kameyama, and K. I. Yamagushi. Subspace identification for continuous-time stochastic systems via distribution-based approach. *Automatica*, 38(1):63–79, 2002.
- [14] Y. Ohta. Realization of input-output maps using generalized orthonormal basis functions. *Systems & Control Letters*, 22(6):437–444, 2005.
- [15] Y. Ohta and T. Kawai. Continuous-time subspace system identification using generalized orthonormal basis functions. In *16th International Symposium on Mathematical Theory of Networks and Systems, Leuven, Belgium*, 2004.
- [16] M. Tischler and R. Remple. *Aircraft And Rotorcraft System Identification: Engineering Methods With Flight-test Examples*. AIAA, 2006.
- [17] P. Van Overschee and B. De Moor. Continuous time frequency domain subspace system identification. *Signal Processing*, 52(2):179–194, 1996.
- [18] M. Verhaegen. Identification of the deterministic part of MIMO state space models given in innovations form from input-output data. *Automatica*, 30(1):61–74, 1994.
- [19] M. Verhaegen and P. Dewilde. Subspace model identification, part 1: output error state space model identification class of algorithms. *International Journal of Control*, 56(5):1187–1210, 1992.
- [20] M. Verhaegen and P. Dewilde. Subspace model identification, part 2: analysis of the elementary output error state space model identification algorithm. *International Journal of Control*, 56(5):1211–1241, 1992.
- [21] B. Wahlberg. System identification using Laguerre models. *IEEE Transactions on Automatic Control*, 36(5):551–562, 1991.
- [22] B. Wahlberg and P. Mäkilä. On approximation of stable linear dynamical systems using Laguerre and Kautz functions. *Automatica*, 32(5):693–708, 1996.
- [23] K. Zhou, J. Doyle, and K. Glover. *Robust and optimal control*. Prentice Hall, 1996.